Soot Volume Fraction Characterization Using the Laser-Induced Incandescence Detection Method

David R. Snelling, Gregory J. Smallwood, and Ömer L. Gülder

National Research Council Canada
ICPET Combustion Research Group, Building M-9
1200 Montreal Road
Ottawa, Ontario K1A 0R6
Canada

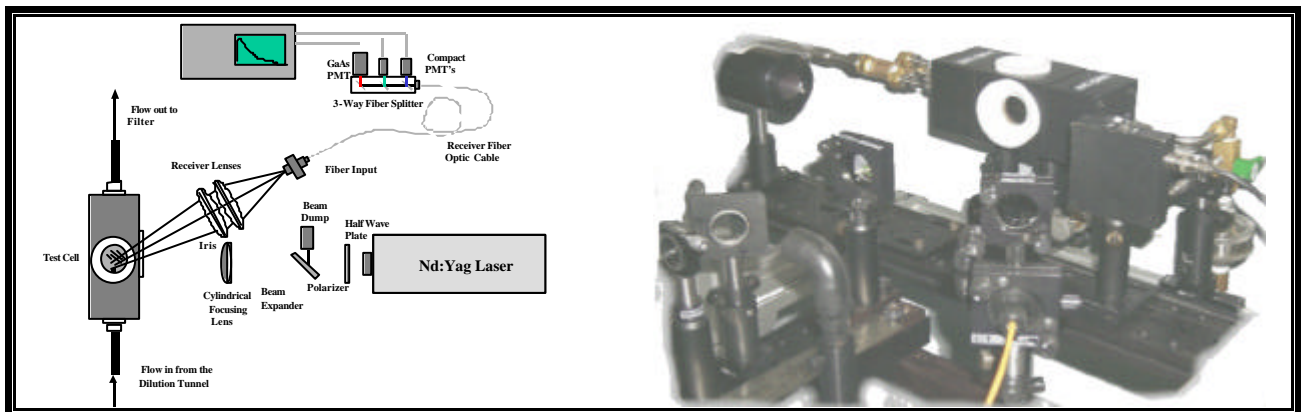**William D. Bachalo and Subramanian Sankar**

Artium Technologies
150 W. Iowa Ave., Suite 101
Sunnyvale, CA, 94086
USA

ABSTRACT

The need is demonstrated for a method and apparatus that measures particulate concentration and primary particle size, that is spatially and temporally resolved, that is capable of real-time measurement and analysis, and that has high sensitivity, wide measurement range, and wide dynamic range, with laser-induced incandescence offering the required capabilities.

The state-of-the-art in LII methodology is briefly reviewed. Details on the effects of laser fluence spatial profile and the effects of the temporal laser fluence distribution are presented, demonstrating the significance of the spatial profile on the excitation curve, and the temporal distribution on the particle temperature and size. The usefulness of LII as a diagnostic instrument for the precise measurement of particulate concentration and primary particle size is demonstrated. Measurements were performed in laminar diffusion flames, the exhaust of a single cylinder DI research diesel engine, and with carbon black.

The use of three wavelength detection to determine particle surface temperature, combined with absolute sensitivity calibration, provides a sensitive, precise, and repeatable measure of the particulate concentration over a wide dynamic range. The LII technique produces good correlation with the gravimetric filter method measurements in the diesel engine exhaust on a mode-by-mode basis over a wide range of operating conditions. The primary particle size can be determined from the LII signals, and the method is precise enough to distinguish particle sizes for different operating conditions in a diesel engine. Once the particulate concentration and primary particle size are known, it is possible to determine the number density of primary particles.

1. INTRODUCTION

There is an urgent need to decrease the total emissions from combustion systems. This requirement is driven by a fundamental desire to preserve our health and the environment and it is being enforced by recent environmental standards and regulations. The undesirable exhaust emissions include CO, NO_x, SO_x, unburned hydrocarbons, and particulate matter. Particulate matter is now receiving greater attention as a pollutant. Efforts have focused on reducing the mass of the combustion-generated particulates in the larger PM_{10} size range (weight of particulate mass below 10 µm aerodynamic diameter) which were visible and hence, readily associated with emissions at the source. However, especially deleterious are the remaining small sized respirable aerosols and particulate matter that are known to produce adverse health effects and are suspected of producing high altitude clouds which adversely affect the earth's climatology. $PM_{2.5}$ range (weight of particulate mass below 2.5 µm aerodynamic diameter) particulates have recently been advanced as the regulatory standard in the U.S. Future regulations may be established for $PM_{1.0}$. It is known that particles in the 0.3 µm size range deposit in the lungs and particles smaller than 0.3 µm find their way into the alveoli. Irrespective of their chemical composition, recent evidence indicates that these fine particles have harmful effects. Vehicle emissions data show that the majority of the particles fall in the range of 0.1 µm. Besides environmental and health concerns, there is also a strong need to control soot and other particulates in the exhaust plume because of their adverse influence on the performance of the power generation systems.

To develop processes and techniques for limiting the emission of soot, we must first possess suitable means for reliably measuring various soot-related parameters. These methods must have adequate dynamic range in order to be able to monitor and characterize the pollutant emissions over a very wide range of concentrations and must operate under a range of environmental conditions from *in situ* exhaust to atmospheric monitoring. In the case of particulate matter, information on the particle mass, size, and volume fraction is needed. The lack of availability of suitable diagnostics has resulted in a degree of uncertainty in the correlation of the particulate loading with health effects. Improvements in the instrumentation are needed to help in developing the test protocols, standards and regulations that will preserve the environment and limit risks to health.

Currently, the Scanning Mobility Particle Sizer (SMPS) is the method considered to be appropriate for measuring the particle size distribution in vehicle emissions. Unfortunately, the method requires extraction and sampling of the exhaust, dilution of the sample, and its operation is repeatable and reliable only under steady-state conditions. Condensation nucleus counters (CNCs) with pre-impactors are used to make coarse estimates of the size of particles above and below a set size (e.g. 0.3 µm). This method also requires sampling and a significant dilution of the sample (on the order of 1000:1) which can lead to errors in the measurements. Because of the complex nature of the particle morphology, particle size or more accurately, the aerodynamic particle size measurements have been made using differential mobility particle sizers (DMPS). In this device, the particles are charged using an electric field and separated by size. The particles separated into classes are then counted using a condensation nuclei counter (CNC) to produce a number-weighted size distribution. Another related approach for measuring particles in the size range of 0.05 to 10 µm is the electrical low-pressure impactor (ELPI). With this instrument, the particles are first charged and then passed through a cascade impactor to segregate them into bins or size classes. The current deposited on each stage of the impactor may be related to the particle concentrations in the various size classes. These methods are useful but leave a degree of uncertainty due to the sampling process and through transport of the particle samples to the device. Gravimetric techniques are considered to be acceptable methods for characterizing the total particle loading. However, the methods do not provide information on the size distribution, require significant sampling times at low particle concentrations, are very time consuming, and are often unreliable because filters do not discriminate particulate matter from other condensed material.

Laser-induced incandescence (LII) measurement is an emerging technology that promises to be a reliable means for spatially and temporally measuring the soot volume fraction and primary soot particle size. Eckbreth (1977) recognized the concept while working with Raman spectroscopy in flames and was troubled by the presence of soot particles that produced laser-modulated incandescence, which could overwhelm the signals desired in the Raman measurements. He was able to relate the time dependence of this interference to laser particulate heating, heat transfer to the medium, particle vaporization, and indirectly to the particle size. Melton (1984) performed numerical calculations to investigate the possibility of developing a soot diagnostic based on this laser heating of particles. He concluded that it might be possible to obtain the particle temperature, soot primary particle size distribution parameters, and relative soot volume fraction. Dasch (1984) modeled the vaporization of small soot particles and conducted experiments demonstrating the method. Since that time, a number of research teams have investigated the method with varying degrees of success (Bengtsson and Alden, 1989; Dec *et al.*, 1991; Quay *et al.*, 1994; Vander

Wal and Weiland, 1994; Bengtsson and Alden, 1995; Will *et al.*, 1995; Mewes and Seitzman, 1997; Snelling *et al.*, 1997). Dec, et al. (1991) used the incandescence method to visualize the soot production inside a diesel engine.

With the LII method, the soot within the laser beam path is heated rapidly using a pulsed laser source with duration typically less than 20 ns (FWHM). The soot is heated from the local ambient soot temperature to the soot vaporization temperature (approximately 4000 to 4500 K). The incandescence from the soot particles is measured using collection optics and photodetectors. Using appropriate calibration and analysis of the incandescence signal, information on the soot volume fraction and primary soot particle size may be obtained. Laser energy absorption by the soot particles and the subsequent cooling processes involve complex analysis of the nano-scale heat and mass transfer in time and space. The method is nonintrusive and is capable of making *in situ* measurements over a very large range of soot concentrations in both flames and under ambient conditions. However, it is not completely non-perturbing as the laser heating can be expected to affect the soot morphology (Vander Wal *et al.*, 1998).

A brief review of the recent work on the method will be provided to establish the state-of-the-art in the methodology. The capability of measuring the soot volume fraction and the soot primary particle size will be demonstrated by comparison to line-of-sight extinction, gravimetric methods, and through comparison to TEM results.

2. DESCRIPTION OF METHOD

2.1 Background

Significant effort has been expended in an effort to characterize soot using optical diagnostics. Much of the earlier light scattering work treated the soot as equivalent spheres to which Mie theory was applied. However, soot particles are generally an aggregation of primary spheres (see Figure 1) with diameters less than about 60 nm which can be described by fractal theories. Another problem is that the complex index of refraction of soot is not known with adequate certainty. Light scatter detection systems using near forward angle detection were argued to be relatively insensitive to the shape of the particles. Although this may be true for particles that do not have large aspect ratio, the long chain-like structures of the soot aggregates (Figure 1) do not meet this criterion. The aggregates may vary in size from a few primary particles to equivalent diameters of 0.5μm. In addition, the near-forward scattering methods using single particle counting experienced problems with high soot concentrations.
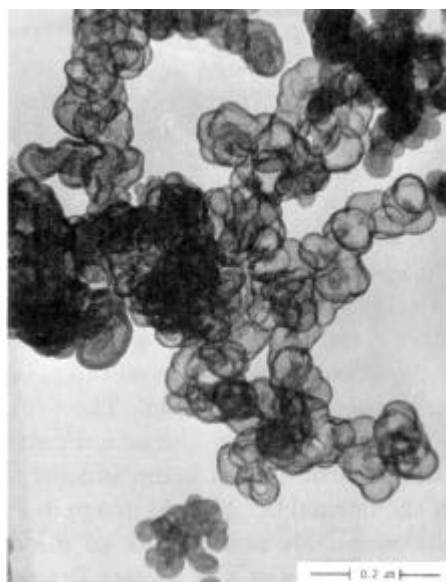

Fig. 1.   Soot particle micrograph from Hess and Herd (1993).

A good review of the soot formation process and the nature of soot is provided by Gülder (1999). Electron microscopy observations indicate that the smallest of the primary particles is approximately 1.5 nm in diameter. The primary particles are then believed to increase in size through a surface condensation of molecules from the gas phase, which results in surface growth. What is referred to as a soot particle size is generally the coagulation of the primary particles into larger aggregates.

A useful summary of the soot morphology and optical properties including a discussion of the Rayleigh-Debye-Gans (RDG) light scattering model and the aggregation of soot may be found in Faeth and Köylü (1995). They recognized that soot consists of nearly spherical primary particles having diameters generally less than 60 nm, which agglomerate into open structured aggregates. These aggregates grow to a wide range of sizes with the largest of the aggregates containing thousands of primary particles resulting in soot aggregate sizes of several microns in equivalent diameter. They also review the scattering models of polydisperse fractal aggregates (PFA) using the RDG approximations. An important observation regarding the formation of the soot aggregates is that the primary particles of soot tend to be bridged rather than just touching spheres indicating subsequent soot growth after aggregation. This indicates that the soot aggregation occurred *in situ* and not due to the sampling process. The open structure of the soot aggregates led to the conclusion that they cannot be modeled as equivalent spherical objects. This observation was made by Snelling et al. (1997) in which they concluded that the equivalent sphere approach was faulty and that the soot particles need to be modeled as aggregates of N_p primary particles of diameter d_p that are just touching. Faeth and Köylü (1995) point out that soot has the physical properties of carbon blacks but with significant porosity. Soot from some internal combustion engines may also contain significant levels of volatile matter. This information is important to the comparison of the LII and the gravimetric methods.

The primary particles of soot at given flame conditions have been recognized by a number of authors as being nearly monodisperse. The size of the primary particles varies with flame conditions and the fuel type with the largest particles being associated with the heavily sooting fuels. The aggregate particle sizes, unlike the primary particles, vary over a large range with relatively broad size distributions. When using the RDG model, the major assumptions noted by Faeth and Köylü (1995) concerning the soot physical properties are as follows: the primary particles are spherical with monodisperse diameter distributions, primary particles just touch each other, they are homogeneous with uniform refractive index, the aggregate size distributions follow a log normal distribution, and the aggregates behave as mass fractal-like objects.

The absorption cross section of laser radiation by soot is proportional to the refractive index function, $E(m)$. Thus, it is $E(m)$ which must be known to model laser heating of the soot particles. A specific knowledge of the complex refractive index is not essential. Gravimetric calibration of the dimensionless extinction coefficient for soot produced by burning crude oil (Dobbins *et al.*, 1994) and acetylene (Choi *et al.*, 1995) gave almost identical values. Wu et al. (1996) measured both the dimensionless extinction and the soot scattering and were thus able to determine $E(m)$ directly. They found that $E(m)$ was independent of fuel type for a range of gaseous and liquid fuels and was also independent of wavelength over the range 400 nm to 800 nm. Their dimensionless extinction coefficients around 5 were somewhat lower than those of Choi, et al. (1995) and Dobbins, et al. (1994) who obtained dimensionless extinction coefficients in the range 8-9. In a subsequent detailed study this same group (Krishnan *et al.*, 2000) is now observing dimensionless extinction coefficients in the same range as those of Choi, et al. and Dobbins, et al., and values of $E(m)$ of approximately 0.3 throughout the visible wavelength range. An alternative approach is to deduce $E(m)$ from refractive index measurements. Smyth (1996) has reviewed much of the information on soot refractive index, for which there is a large spread of values. The refractive index data and that of Dalzell and Sarofim (1969) and Stagg and Charalampopoulos (1993) give a value of $E(m)$ in reasonable agreement with the scattering/extinction studies. Overall one can conclude that $E(m)$ is in the range 0.2 to 0.3, largely independent of wavelength in the visible.

Santoro and his co-workers (Quay *et al.*, 1994) obtained spatially resolved soot volume fraction measurements using a combination of light scattering/extinction techniques on a sooting laboratory flame. They were able to use combined light scattering and LII to obtain spatially resolved measurements of number concentrations and particle sizes. Ni, et al. (1995) pointed out that with a variation in laser fluence, the decay constant of the LII signal varies significantly. Their conclusion was that such a dramatic effect could not be explained by reduction in the soot particle size alone and that it may be due to significant changes in the soot morphology. However, the authors were only looking at delay times up to approximately 100 ns where vaporization is expected to be the dominant heat loss mechanism. In addition, the experiments included fluence values where vaporization temperatures were not reached.

A number of papers by Vander Wal and colleagues (Vander Wal and Dietrich, 1994; Vander Wal and Dietrich, 1995; Vander Wal *et al.*, 1996; Vander Wal *et al.*, 1997; Vander Wal and Jensen, 1998; Vander Wal *et al.*, 1998) consider LII processes, particularly the morphological changes that occur with rapid heating of soot. Vander Wal and Weiland (1994) recognized that the LII signal is unaffected by the elastic light scattering contributions that affect the light absorption measurements of large soot aggregates and the uncertainties in the complex refractive indices. They pointed out that the LII signal depends upon 1) the excitation and detection wavelengths, 2) the excitation intensity, 3) detection timing and duration, and 4) the soot volume fraction. Vander Wal, et al. (1996)

used gravimetrically determined soot volume fractions to calibrate the LII method and demonstrate the linearity of the LII calibration over a range of volume fractions from 0.078 to 1.1 ppm.

An investigation of the effects of the rapid heating of soot, which has the potential of producing chemical and physical changes in the soot and raises questions as to how the LII signal may be affected by these changes was conducted by Vander Wal (1995). TEM micrographs were obtained of soot samples for soot not irradiated by the laser and for soot collected using thermophoretic sampling after irradiation with the pulsed laser. The latter showed unusual shell structures. For some of the soot particles, apparent small structures within the shell were observed whereas other particles appeared to have voids or porous material in the inner core. Adjacent particles were observed to show a more normal morphology. They demonstrated with the use of X-ray analysis that the shell structures were soot not some contaminant material.

Several studies have been conducted to determine whether the primary soot particle size may be determined using LII. The theory indicates that the decay of the signal after excitation may be related to the primary particle size since the cooling of the particles is predominantly through conduction and convection, which is dependent on the surface area. Vander Wal, et al. (1999) and Mewes and Seitzman (1997) proposed two methods based on a theoretical model for obtaining the particle size information. One method used the ratio of the signal intensity at two wavelengths integrated over the same time delay and duration after the laser pulse. The second method used the same averaged temporal curve at a single detection wavelength with a gate ratio formed at two different delays after the laser pulse. The results were compared to thermophoretic sampling with subsequent TEM microscopy observations. Concerns were expressed over the fact that in regions of the flame, the aggregates become larger and more dense and compact. Changes in the aggregate structure can be expected to cause a decrease in the cooling rate of the individual primary particles. Nonetheless, good agreement was achieved in certain regions above the burner face.

Vander Wal and Jensen (1998) investigated the effects of laser fluence upon the LII signal and the potential for the heating to change the soot morphology and properties. The laser light fluence used is generally established empirically by observing the LII signal which increases rapidly, then becomes nearly constant, and then decreases with increasing laser fluence. The laser fluence is chosen for the plateau region observed from the signal. The authors indicate that several physical processes are hidden in this signal behavior. Their data and TEM images suggest that dramatic changes are taking place in the soot morphology during laser light heating. The temporal decay rate of the signal increases while the peak intensity increases with increase in laser fluence. The outcome integrated over the detector gate time is a nearly constant signal for a range of fluence. The laser-heated particles have a higher rate of cooling since the surface area to solid volume ratio is greater for hollow spheres than for solid particles. At laser light fluence greater than 0.5 J/cm^2, the peak signal intensity was observed to decrease since the temporal decay rate of the incandescence continues to increase due to the morphology change in the soot and significant increase in the soot vaporization rate takes place.

Soot primary particle size measurements were attempted by McManus, et al. (1998) using the LII method and SEM micrographs for comparison. Two flames were used with equivalence ratios of 1.5 and 1.8. A set gate width was used to measure the incandescence signal at delays from 0 to 1.1 μs from the trailing edge of the laser light pulse. The cooling rates predicted using the heat transfer model were used to obtain primary particle size from the LII signal decay rate. The model predicted particles in the size range of 30 and 40 nm in diameter for the equivalence ratios of 1.5 and 1.8. The SEM micrographs showed primary particle sizes to be approximately 20 and 40 nm in diameter. At higher particle temperatures, they found a discrepancy in the vaporization-dominated regime. The authors concluded that there may be a change in the soot properties due to excessive heating.

Will et al. (1998) provide an analysis of the factors affecting the performance of the LII method for particle sizing. An attempt was made to show how the ratio of the LII signal at two delay times could be used to determine the primary particle size. The assumption was made that the primary particles are spherical and form aggregates of varying and unknown size. Absorption of light and emission of radiation was assumed to be from independent primary particles since the soot aggregates have been observed to be loosely structured aggregates with fractal dimensions in the range of 1.5 to 1.8. The authors argue that the laser Gaussian intensity profile does not present a significant problem since the error in the determination of the particle size is almost linearly dependent on the deviation from the nominal laser irradiance over a fairly wide range.

Arguments have been made by Will et al. (1998) and Mewes and Seitzman (1997) regarding the effects of the particle vaporization to address the fact that the heat of vaporization and the vaporization temperature are subject to large uncertainties. Will et al. (1998) indicate that these parameters do not affect the cooling mechanisms for the LII time scales used but determine only the shrinkage of the soot particles. The authors claim that since the heat

conduction is proportional to the difference between the particle and the surrounding gas temperature, there must be a significant influence of the gas temperature, T_0 on the accuracy of the particle size determination. Some concern has been expressed regarding the shape and contact area of touching neighboring particles. The shape of the primary particles was shown previously to have a significant effect on the signals. It was also recognized that the particle heat conduction surface is reduced by approximately 10% from that of an isolated sphere due to touching neighboring particles. The heat loss will also depend on where the sphere is within the aggregate. Concern also has been expressed about the mutual interference of the heat loss of individual particles.

The theoretical heat transfer model has been described in detail elsewhere (Snelling *et al.*, 2000a), and common errors made in application of the model have recently been summarized (Smallwood *et al.*, 2000).

2.2 Particulate Concentration

In the past, quantitative LII determinations of the particulate concentrations have been made relating the intensity of the LII signal to the known particulate volume fraction in a calibration source. More recently, Snelling et al. (2000a) have devised a different approach involving the measurement of the particulate surface temperature using three-wavelength pyrometry. The first step in the process is to calibrate the system using a single point incandescence measurement of a known source at a predetermined temperature, which provides an absolute sensitivity of the detection system in $W/m^3 \cdot ster$. The particulates are first heated to their incandescence temperature using a pulsed laser source (1064 nm wavelength) and the time-resolved incandescence is recorded at three wavelengths. The particle temperature may be obtained from the ratio of the measured incandescence detected at any two wavelengths using the following expression

$$\frac{I_{\lambda_1}}{I_{\lambda_2}} = \frac{\lambda_2^6 \left(e^{hc/k\lambda_2 T} - 1 \right)}{\lambda_1^6 \left(e^{hc/k\lambda_1 T} - 1 \right)} \frac{E(m)_{\lambda_1}}{E(m)_{\lambda_2}} , \tag{1}$$

where λ is the detection wavelength, h and k are the Planck and Boltzman constants, c is the speed of light, T is the particle surface temperature, I_λ is the incandescence intensity, and $E(m)$ is a particle refractive index dependent function. Based upon the commonly accepted refractive index for soot of $m = 1.57 + 0.56i$ (Dalzell and Sarofim, 1969), $E(m)$ is assumed to have the value 0.26 for the wavelengths of interest. $E(m)$ appears as a ratio at different wavelengths and T appears in the exponential function in the above equation so the deduced particle temperature T tends to be insensitive to variations of $E(m)$ with detected incandescence wavelength. For example, an increase or decrease in $E(m)$ of 10% results in a corresponding increase or decrease of only 2.5% in the estimated temperature. The absolute value of $E(m)$ appearing in the next equation is significant since there is a proportional dependence on the estimated particle incandescence.

Using the particle surface temperature and the accepted value of $E(m)$, the incandescence from a primary particle of diameter d_p can be determined from

$$P_p(\lambda) = \frac{8\pi^3 c^2 h}{\lambda^6 \left(e^{hc/k\lambda T} - 1 \right)} d_p^3 E(m) . \tag{2}$$

The measured incandescence intensity is divided by the predicted incandescence for a single primary particle, P_p, to determine the number N_p of primary particles within the sample volume during the measurement. Particulate volume fraction (PVF) can then be determined from the following expression

$$PVF = \frac{\pi d_p^3}{6} \frac{N_p}{V} , \tag{3}$$

where V is the measurement or sample volume defined by the cross-sectional area of the laser sheet observed by the light collection optics and the effective laser light sheet thickness. It should be noted that N_p depends on $I_\lambda / P_p(\lambda)$ and hence, on $1/d_p^3$. Thus, PVF is independent of the assumed primary particle size.

2.3 Primary Particle Size

At some time after the laser excitation, the dominant cooling mechanism for the particle becomes conduction to the surrounding gas. During the conduction phase, the difference between the particle surface temperature and the ambient gas temperature decays steadily in an exponential manner. An equation of the form

$$\Delta T = A e^{-\Delta t / \tau} , \tag{4}$$

where A is a constant, is fit to the temperature data to determine the characteristic decay time, τ. Since the heat transfer by conduction depends on the temperature difference between the particle surface and the ambient gas, the gas temperature must also be known. The gas temperature may be determined from thermocouple measurements or other means. The relationship between particle size and the characteristic time of the exponential decay is shown in Figure 2 for a range of sizes expected for primary particles.
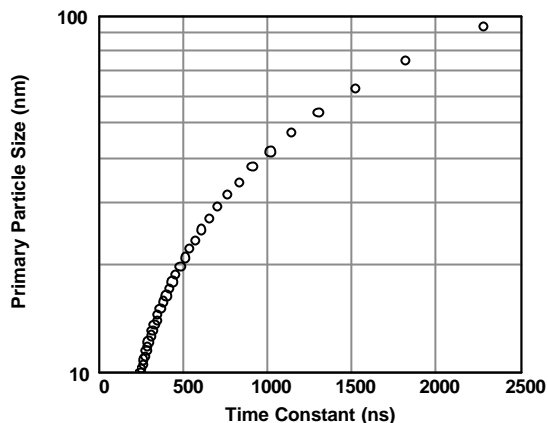
Fig. 2.   *Primary particle size as determined from the characteristic time of the exponential decay of the temperature difference between the particle surface and the ambient gas.*

With determination of τ, the primary particle diameter may be inferred from the expression (McCoy and Cha, 1974)

$$d_p = \frac{12 k_g \alpha}{G \lambda_{MFP} c_p \rho_p t},$$ (5)

where k_g is the thermal conductivity of the ambient gas, α is the accommodation coefficient equal to 0.26, G is the geometry-dependent heat transfer coefficient, λ_{MFP} is the molecular mean free path in the ambient gas, c_p is the specific heat of the particle material, and ρ_p is the density of the particle. The primary particle size is obtained under the assumptions of just touching spheres of nearly monodisperse homogeneous primary particles with uniform refractive index.

3.   EXPERIMENTAL APPARATUS

3.1 General Description

The basic experimental requirements for producing an LII signal are a pulsed laser beam to heat the particulates, a photodetector to measure the radiation, and a recording device to measure the photodetector output. Application of an Nd:YAG laser operating at its fundamental wavelength of 1064 nm offers the likelihood that all the primary particles will be in the Rayleigh regime, which is assumed in the LII theory, and it avoids possible interference effects such as exciting PAH fluorescence or C_2 emission. A half-wave plate (to rotate the plane of polarization) in combination with a thin film polarizer (angle-tuned to transmit horizontally polarized radiation) may be used to limit the laser energy.

As discussed above, use of a uniform beam profile is ideal as all the particulates in the probe volume are then exposed to the same level of laser fluence. Such a profile is difficult to achieve. However, employment of a mini-sheet provides a nearly uniform profile in at least a two-dimensional plane through the same volume. Use of a lens in the detection arm increases the signal collection efficiency, and insertion of an aperture provides a well-defined probe volume. Narrowband interference filters provide wavelength discrimination. Photomultipliers supply the appropriate combination of time response, spectral response, dynamic range, and sensitivity required for LII. The time dependent signal, its peak, or an integration of the signal presents the information necessary to determine the particulate concentration. A transient digitizer or a gated integrator typically records the signal. Use of a transient digitizer is warranted for the measurement of primary particle size, as it is often determined from the decay of the signal. For steady-state operating conditions, acquisition of a multipulse average signal is recommended, to reduce the noise in the signal.

7

3.2 Apparatus for Evaluation of the LII Method

The LII system was originally evaluated by measuring soot concentration in a laminar diffusion flame (Snelling *et al.*, 1997), where high spatial resolution was required due to the highly annular structure of the soot-bearing regions. The laminar diffusion flame studied in these experiments was an ethylene/air coflow flame with a visible flame height of 67 mm. The detection arm was orthogonal to the direction of beam propagation, as shown in Figure 3. The LII signal from the center of the laser sheet was imaged onto apertures in front of the photomultipliers, resulting in a cylindrical probe volume with a diameter of 0.53 mm and length equal to the width of the laser sheet (0.44 mm), as measured with a Coherent BeamView system. The interference filters were centered at 455 nm, to minimize the effects of flame radiation. The peak and integrated signal intensities were measured with gated integrators, the latter made available by inserting a charge-coupled amplifier between the photomultiplier and the gated integrator.
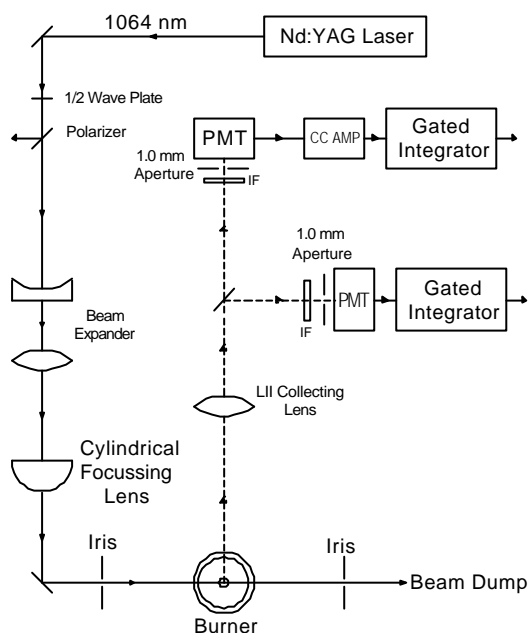

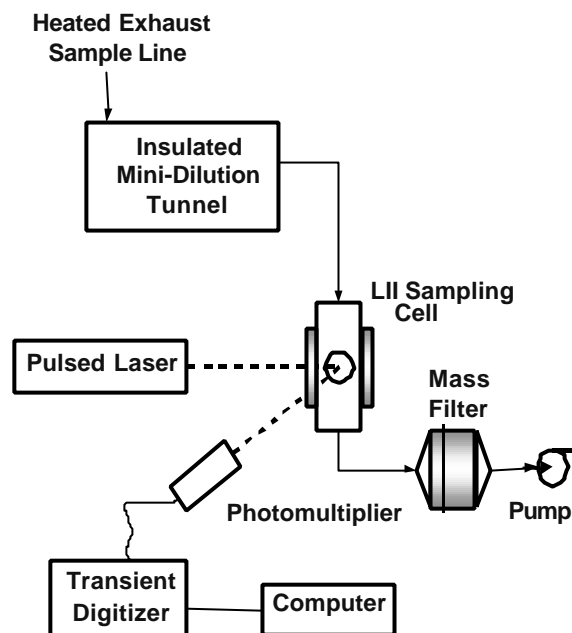*Fig. 3.   Schematic of the LII apparatus for measurements in the laminar diffusion flame (Snelling, et al., 1997).*

Fig. 4.   Schematic of the LII apparatus for measurements of the particulate matter in the diesel exhaust (Snelling, et al., 1999a, Snelling, et al., 2000a).

3.3 Apparatus for Measurement of Particulate Matter in Diesel Exhaust

The measurement of diesel exhaust particulate matter (Snelling *et al.*, 1999a; Snelling *et al.*, 2000b) imposed further constraints, requiring the apparatus to be substantially modified. Simultaneous LII and EPA standard gravimetric measurements of the particulate loading was required for direct comparison of the two techniques. This necessitated the insertion of an optically accessible cell in the tube leading from the exhaust dilution tunnel to the filters, as shown in Figure 4. This cell provided a window for introducing the laser beam and for signal collection, a second window for passing the laser beam to a beam dump, and a third window orthogonal to the laser beam for viewing and alignment. The laser sheet was centered 2 mm from the open end of the tube carrying the exhaust from the dilution tunnel. The Nd:YAG laser was operated with 15 mJ/pulse at 20 Hz and 1064 nm. The beam was then focused with a cylindrical lens to form a sheet through the probe volume. The beam energy profiles in the probe volume were measured with a Coherent BeamView system. These profiles were used to ensure that the laser fluence throughout the probe volume was just beyond the saturation threshold for raising most of the soot particles to the evaporation temperature.

As the concentration of particulates in the flow was orders of magnitude less than those measured in the laminar diffusion flame, and the concentration was considered to be uniform across the tube, the probe volume was expanded to generate and collect more incandescence signal. Normally, dilution would not be used for the LII method, but was necessary for the gravimetric protocol. The optimum configuration for the instrumentation required the excitation and signal beams to pass through the same window. Thus, the imaging system was arranged such that

the imaging axis was at an angle of 35° to the plane of the laser sheet (Figure 4). The probe volume in the cell was a slanted cylinder of diameter 1.2 mm and 2.1 mm mean length.

The LII signal from the mid-height of the laser sheet was imaged onto an optical fiber which transmitted the incandescence signal to the photomultipliers. For the three-wavelength pyrometry used to determine the particulate surface temperature, the LII signal was recorded by three photomultipliers, equipped with narrowband interference filters centered at 400 nm, 550 nm, and 780 nm, respectively. Transient signals from the photomultipliers were recorded at 2 ns resolution and subsequently transferred to a computer for further analysis. Multipulse averages were acquired, with a minimum of 400 samples per average. 5 of these averages were collected during each trial, and three trials were performed for each of the eight engine operating modes evaluated.

3.4 Apparatus for Measurement of Carbon Black

The LII system for the measurement of primary particle size from various carbon black powders was identical to the system used for the diesel exhaust measurements, without the optical sampling cell. The carbon black particles were suspended in an ethanol solution which was sprayed through an airblast medical nebulizer. The droplets were carried into a heated chamber, where the methanol evaporated and additional air was supplied. The carbon black particles were dispensed through a contracting nozzle at the exit of the chamber.

4. RESULTS

4.1 Typical LII Signals

An example of transient LII signals is shown in Figure 5. These signals were recorded as a function of time, capturing not only the peak signal but also the decay of the signal as the particles cool to the ambient temperature. The three curves represent the data simultaneously acquired at the three wavelengths. The data has been time-averaged to reduce the number of data points at long times, where the signal is changing slowly. The magnitude of the signal has been corrected for any background offset. The timebase for the three wavelengths has been adjusted to compensate for variation in the lengths of cable and fiber, and the time constants of the photomultipliers have been found to be similar, so that the relative time between the signals is correct, but the absolute time scale is arbitrary and the Q-switch pulse does not necessarily begin at 0 ns. Calibration of the detection system allows conversion of the photomultiplier signals into absolute spectral intensity.

As would be expected, the longest wavelength (780 nm) channel was the first to rise following the beginning of the laser pulse, and was the slowest to decay. It was followed by the middle (550 nm) and shortest wavelength (400 nm) channels. This was due to the shift towards blue wavelengths as black-body emitters increase in temperature. Further investigation of Figure 5 shows that after 600 ns, the signals have dropped 3 to 4 orders of magnitude from the peak values, and the noise level becomes significant.

4.2 Effects of Laser Fluence Spatial Profile

Snelling, et al. (1997) recognized that the spatial energy profile of the laser beam should be accounted for in the analysis. The calculated signal intensities, $I(\lambda,t)$ must be integrated over the range of fluence across the laser beam. For a one-dimensional Gaussian profile produced by a laser light sheet, this can be described as

$$F(x) = F_o \exp\left(-x^2 / w_x^2\right),$$ (6)

where w_x is the $1/e^2$ half width sheet thickness and F_o is the peak fluence in the probe volume at the center of the sheet. Although it has been argued that the fluence and hence the Gaussian beam intensity or fluence profile does not affect the results, the experimental data show this not to be true. The results indicate that the excitation curve (LII signal as a function of laser fluence) is strongly dependent on the spatial laser intensity distribution, Figure 6. Experimentally, the strong effect of the spatial laser intensity distribution on the excitation has been observed by Ni et al. (1995). A similar finding has also been demonstrated theoretically by Tait and Greenhalgh (1992; 1993) for rectangular and Gaussian laser beams. The physical reason behind this strong dependence has been discussed by Snelling et al. (1997; 2000a).

4.3 Effects of Temporal Laser Fluence Distribution

To investigate the effects of the temporal laser intensity distribution, Snelling et al. (2000a) considered three temporal profiles for an identical laser fluence of 0.725 J/cm² with uniform spatial distribution. These were the

standard Q-switch profile from a Nd:YAG laser with a duration of 7 ns FWHM, and two triangular profiles with durations of 7 and 14 ns FWHM, respectively. The results showed that the excitation curve is insensitive to the temporal distribution of the laser energy as long as the laser energy is delivered sufficiently rapidly. These results support the suggestion of Shaddix and Smyth (1996) to use laser fluence (J/cm^2) to characterize the laser energy dependence of LII signal instead of laser intensity (W/cm^2).
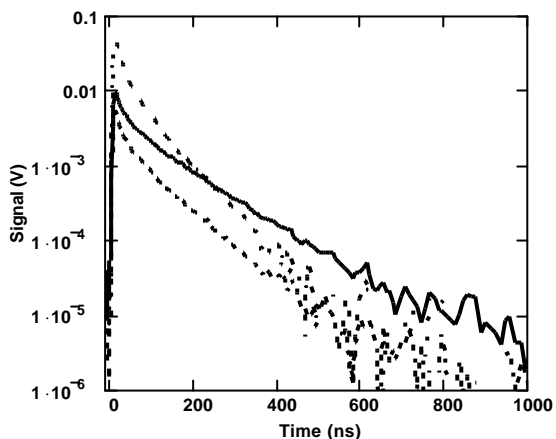
Fig. 5. Typical LII signal (photomultiplier voltage) recorded in a diesel exhaust, with three wavelength detection. (dash-dot line – 400 nm; dash line – 550 nm; solid line – 780 nm)
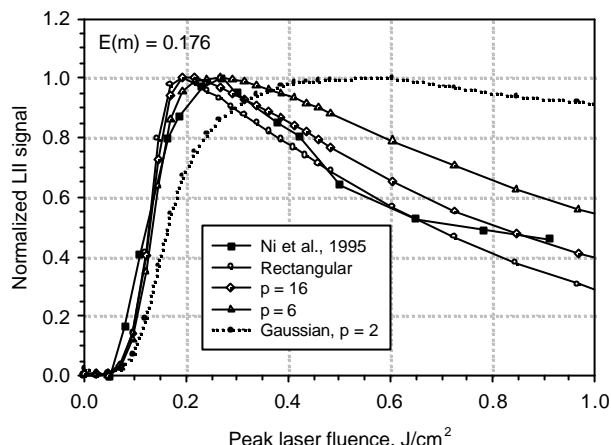
Fig. 6. Effects of the spatial laser intensity distribution on the prediction of the excitation curve.

Although the temporal distribution of the laser energy has only a slight effect on the excitation curve, it has significant impact on the history of the predicted soot temperature and diameter as shown in Figure 7. For a given total laser energy, the shorter the laser pulse, the faster the temperature rise and the higher the peak soot temperature, Figure 7(a). Correspondingly, the shorter the laser pulse, the smaller the soot particle size after the laser pulse, Figure 7(b). It is therefore important to report the temporal distribution of laser energy for the pulsed laser used in LII experiments. Unfortunately, in the LII literature, the excitation source is rarely defined with sufficient detail to allow the experiments to be duplicated or modeled. As a minimum, the spatial fluence profile in the excitation volume and the temporal profile of the laser pulse should be measured and reported.
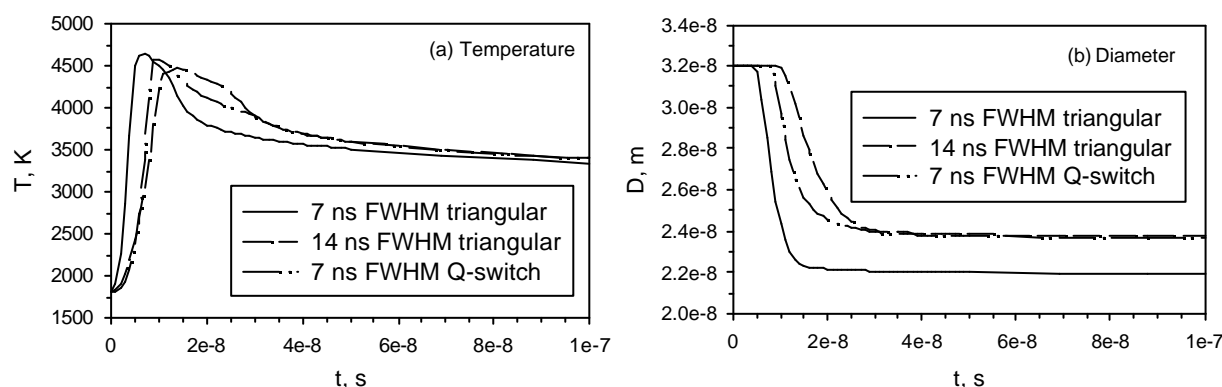

Fig. 7. Effects of the temporal distribution of the laser energy on the predicted history of (a) soot particle temperature and (b) soot particle diameter.

4.4 LII Soot Volume Fraction Measurements

The LII method was evaluated using soot measurements in laminar flames by comparing the measurements to line-of-sight light beam extinction measurements, Figure 8. Using the Abel inversion, the spatial variation of the soot

volume fraction was extracted from two dimensional line-of-sight extinction measurements (Snelling *et al.*, 1999b) and compared with the approximate point measurements obtained with the LII system. In Figure 8 the LII data has been scaled to the Abel data so that the integrated soot volume fraction over the total flame width is the same for all the curves. It can be seen that there is good agreement between the soot profiles from LII and Abel inverted transmission measurements, with the prompt LII data (acquired for 25 ns around the peak) following the Abel inverted data more closely than the integrated signal. Also, the need for high spatial resolution may be observed from Figure 8, as the soot concentration drops from its peak to zero with less than 1 mm radial displacement. In the soot concentration range 0.5-5.0 ppm the prompt LII and the extinction measurements are linearly related, and the agreement is shown to be very good.
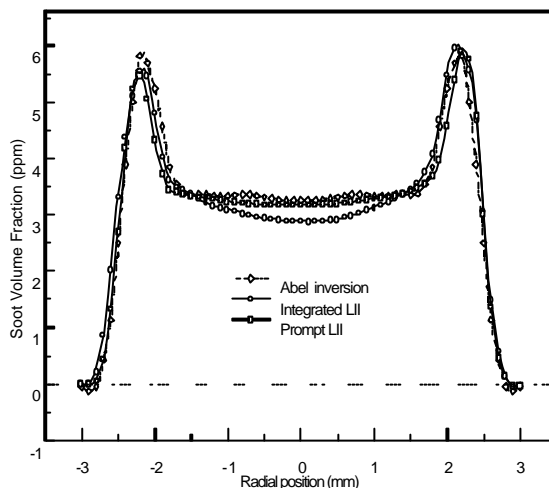

Fig. 8.   Volume fraction comparisons for data obtained with the LII and line-of-sight extinction measurements using the Abel inversion.

4.5 Measurement of Particulate Matter in Diesel Exhaust

Soot volume fraction measurements were also obtained in a diesel exhaust and compared with gravimetric results obtained simultaneously (Snelling *et al.*, 2000b). The optical pyrometry technique was applied to determine the particulate surface temperature throughout the rapid heating due to laser irradiation and subsequent cooling. Peak temperatures of 4400 – 4500 K were typically observed. The LII technique provides a precise measure of the particulate surface temperature from shortly before the peak to when the signal has dropped more than two orders of magnitude, with a typical maximum error of ± 4%. The concentration of particulates for the data shown in Figure 5, determined from the maximum absolute intensity and peak particulate surface temperature, is 3.4 ppb. The linearity of the calibration, a conversion from absolute intensity to particulate concentration, is good as the data is nearly within a single standard deviation of the best-fit line over almost two orders of magnitude.

The particulate concentration data is shown by engine operating mode in Figure 9. The particulate volume fractions reported are for the dilute exhaust, as measured in the sampling cell. As expected, the idle condition (Mode 1) produces the lowest levels of particulates, the low speed, high load conditions (Modes 3 and 4) produce the highest levels of particulates, and the high speed modes (5 – 8) produce moderate levels of particulates. All trials for a given mode produce results that agree within a single standard deviation, and that the greatest variability occurs in Mode 4. Mode 4 also produces the greatest amount of particulates and is the most unstable of the engine modes. The high variability was also observed in the gravimetric results, and is attributed to instability in the engine emissions output.

Comparison of the particulate concentration data obtained from LII via the absolute calibration method is in reasonable agreement with gravimetric data acquired simultaneously, as shown in Figure 10. The largest discrepancies are at the two extremes. In general, the gravimetric method tends to produce higher results for the modes with the lowest particulate concentrations. These are also the modes with the highest fraction of soluble organic fraction (SOF), and thus, much of this discrepancy may be due to components other than dry soot.

It should be noted that in general, detailed analysis is not performed on particulates measurements on a trial-by-trial, or even a mode-by-mode basis. Due to the uncertainties in the acquisition of gravimetric data from the dilution tunnel, often it is only the composite emissions from the full cycle that are reported. For comparison, the engine-out

(undiluted) brake specific emissions (BSE) of particulate matter (PM) are 0.11 g/hp·hr for the LII results and 0.074 g/hp·hr for the gravimetric results.
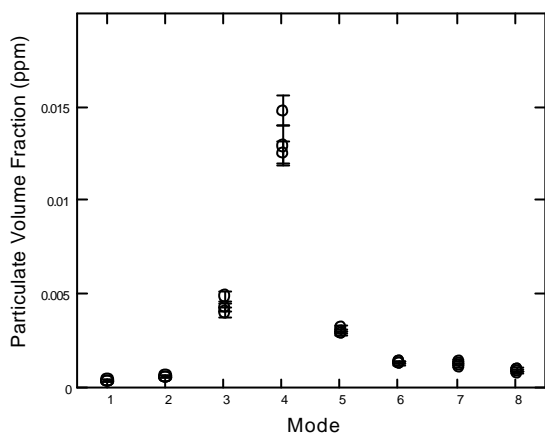

Fig. 9. *Particulate volume fraction by mode. Error bars indicate standard deviation for each of the three trials per mode.*
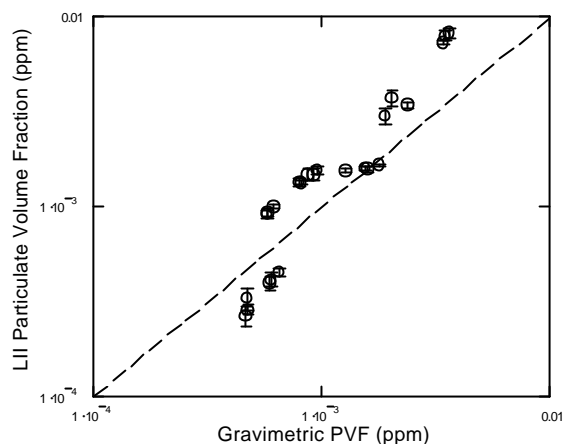
Fig. 10. *Particulate concentration as determined by the LII and gravimetric methods.*

As described above, the primary particle size may be determined from the decay of the LII signals. For each of the engine operating modes, three 1000-pulse averages were acquired. The temperature during the steady phase of the exponential decay was analyzed to determine the primary particle size. A typical example, recorded during a high speed/low load condition, is shown in Figure 11. The agreement between the best-fit exponential decay and the data is exceptional over a time period of several hundred nanoseconds, until the signals have become so weak that the measured temperatures are starting to become unreliable. The diameter determined by the fit to the experimental data in Figure 11was 43 nm.
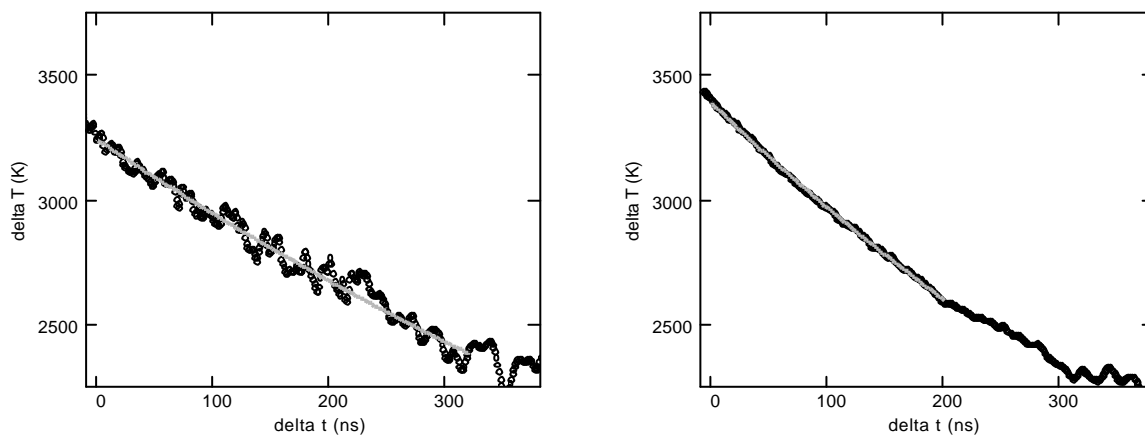

Fig. 11. *Differential between particle surface temperature and ambient temperature during conductive cooling period, for diesel exhaust (left) and carbon black (right). Time scale has an arbitrary origin during the steady exponential decay. Circles represent experimentally derived data, line is best-fit to data.*

The results for primary particle size acquired for all engine modes are shown in Figure 12. From this data it appears that the primary particle size can be reliably determined. Further experiments are required to establish the precision of the technique. The mean particle sizes ranged from 36 nm to 87 nm, with a trend for the larger particles to appear in the low speed, low load modes (Modes 1 and 2) and the smaller particles to appear in the high speed, low load modes (Modes 5 and 6). At high load, the engine speed appeared to have little effect, as the sizes recorded in Modes 3, 4, 7 and 8 were all similar. These sizes are consistent with primary particle size determination from photomicrographs, which indicate diameters from 10 to 80 nm (Amann and Siegla, 1982). The primary particle size determined by LII is linearly proportional to the accommodation coefficient (Snelling *et al.*, 2000a), which was taken as 0.26 (Leroy *et al.*, 1997) for the reported results.
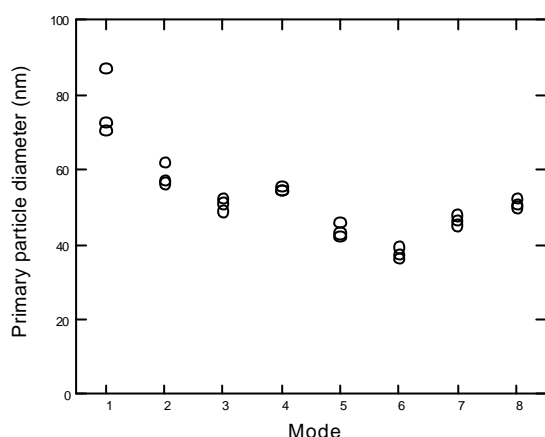
12

Fig. 12. Primary particle diameter measured for each of the eight engine operating modes.
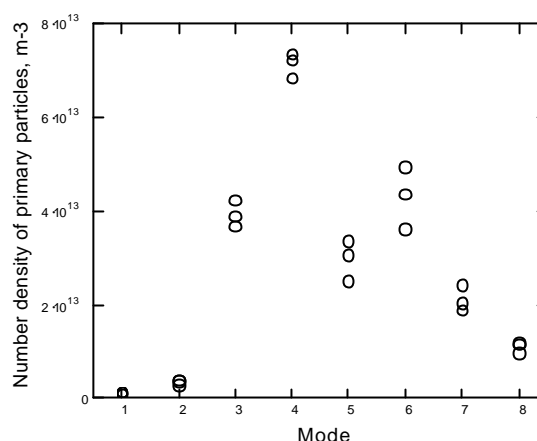

Fig. 13. Number density of primary particles measured in the diluted exhaust for each of the eight engine operating modes.

Combining the primary particle size data (Figure 12) with the measured particulate concentrations in the dilution tunnel (Figure 9), the number density of primary particulates in the dilute exhaust is shown by engine mode in Figure 13. There are two orders of magnitude variation in the number density of primary particles, from Mode 1 (lowest) to Mode 4 (highest). The number of aggregates would be significantly lower, as there are typically tens of primary particles per aggregate.

4.6 Measurement of Carbon Black

Further measurement of primary particle size has been performed with various carbon black powders using the carbon black dispenser described above. The nominal spherule diameters were 13 to 100 nm. Preliminary results have indicated sizes from 20 to 150 nm, about 50 % larger than the specifications for the carbon black. An example of the decay used to determine the primary particle size for the smallest carbon black particles is shown in Figure 11. This discrepancy may be due to the fact that the primary particles are not the assumed just-contacting spheres, but are highly aggregated, with considerable bridging between primary particles, and near-complete shielding of some of the interior particles in the larger aggregates. The specifications for the carbon black are based upon methods that infer the primary particle size, such as with correlations from TEM photographs, or with surface adsorption measurements. Assumptions made in these methods may also account for some of the discrepancy between the specification data and the LII results.

4.7 Discussion

There are many possible reasons for the discrepancies between the LII and gravimetric techniques in the diesel exhaust, which primarily derive from the fact that the two techniques are measuring significantly different aspects of the particulate emissions. Gravimetric sampling includes an organic fraction that does not contribute to the signal measured by LII. The density of the particulates is required to convert the mass determined by the gravimetric filter method to a volume fraction for comparison with LII. A density for dry soot is used, which does not account for the organic fraction, producing another source of error. The repeatability and accuracy of our gravimetric data is compromised by the use of an older dilution tunnel and related instrumentation. We are in the process of upgrading to a modern commercial mini-dilution tunnel, which is anticipated to provide more reliable results. The calculated LII particle intensity is sensitive to errors in the soot surface temperature. The total black body radiation scales as T^4, so that the maximum 4% error in temperature results in a 16% error in intensity. Finally, the particulate volume fraction is inversely proportional to $E(m)$, and thus a 30% increase in $E(m)$ would result in a 30% decrease in the measured PVF. Recent results have indicated that the value of $E(m)$ is higher than previously thought (Krishnan *et al.*, 2000). The LII uncertainty and the known large errors in gravimetric sampling cover the apparent differences between the two techniques. Given the uncertainties in the gravimetric and LII measurements the agreement is very satisfactory.

It must be emphasized that the reported primary particle diameters represent an assumed monosized average over the ensemble of particles in the sample volume and over the number of single-shot measurements recorded.

Ultimately, it is the aggregate size that is of the greatest interest from the health, environment, and regulation perspectives. Further work is planned to determine the aggregate sizes of particulates in diesel exhaust.

5. SUMMARY

The need has been demonstrated for a method and apparatus that measures particulate concentration and primary particle size, that is spatially and temporally resolved, that is capable of real-time measurement and analysis, and that has high sensitivity, wide measurement range, and wide dynamic range, with laser-induced incandescence offering the required capabilities.

The state-of-the-art in LII methodology has been briefly reviewed. Details on the effects of laser fluence spatial profile and the effects of the temporal laser fluence distribution have been presented, demonstrating the significance of the spatial profile on the excitation curve, and the temporal distribution on the particle temperature and size. The usefulness of LII as a diagnostic instrument for the precise measurement of particulate concentration and primary particle size has been demonstrated. Measurements have been performed in laminar diffusion flames, the exhaust of a single cylinder DI research diesel engine, and with carbon black.

The use of three wavelength detection to determine particle surface temperature, combined with absolute sensitivity calibration, provides a sensitive, precise, and repeatable measure of the particulate concentration over a wide dynamic range. The LII technique produces good correlation with the gravimetric filter method measurements in the diesel engine exhaust on a mode-by-mode basis over a wide range of operating conditions. The primary particle size can be determined from the LII signals, and the method is precise enough to distinguish particle sizes for different operating conditions in a diesel engine. Once the particulate concentration and primary particle size are known, it is possible to determine the number density of primary particles.

The LII technique is capable of real-time particulate matter measurements under transient conditions. The wide measurement and dynamic ranges and lower detection limit of LII make it a potentially preferred standard instrument for PM measurements. Further development of the LII technique has the potential to give information about extensive aspects of the morphology of the particulate matter. Use of LII also provides a significant time advantage over the gravimetric procedure and other instruments, both in the collection and processing of data.

REFERENCES

Amann, C. A. and Siegla, D. C., (1982), "Diesel Particulates - What They Are and Why," Aerosol Science and Technology(1): 73-101.

Bengtsson, P. E. and Alden, M., (1989), "Application of a Pulsed Laser for Soot Measurements in Premixed Flames," Applied Physics B (Photophysics and Laser Chemistry) **B48**(2): 155-64.

Bengtsson, P. E. and Alden, M., (1995), "Soot-Visualization Strategies Using Laser Techniques. Laser-Induced Fluorescence in C2 from Laser-Vaporized Soot and Laser-Induced Soot Incandescence," Appl. Phys. B: Lasers Opt **1**: 51-9.

Choi, M. Y., Mulholland, G. W., Hamins, A. and Kashiwagi, T., (1995), "Comparisons of the Soot Volume Fraction Using Gravimetric and Light Extinction Techniques," Combust. Flame **102**(1/2): 161-9.

Dalzell, W. H. and Sarofim, A. F., (1969), "Optical Constants of Soot and Their Application to Heat Flux Calculations," Journal of Heat Transfer **91**: 100-104.

Dasch, C. J., (1984), "New Soot Diagnostics in Flames Based on Laser Vaporization of Soot," 20th Symp. (Int.) on Combustion, 1231-1237.

Dec, J. E., zur Loye, A. O. and Siebers, D. L., (1991), "Soot Distribution in a D.I. Diesel Engine Using 2-D Laser-Induced Incandescence Imaging," SAE Transactions **100**: 277-288.

Dobbins, R. A., Mulholland, G. W. and Bryner, N. P., (1994), "Comparison of a Fractal Smoke Optics Model with Light Extinction Measurements," Atmos. Environ. **28**(5): 889-97.

Eckbreth, A. C., (1977), "Effects of Laser-Modulated Particulate Incandescence on Raman Scattering Diagnostics.," Journal of Applied Physics **48**(11): 4473-4479.

Faeth, G. M. and Köylü, Ü. Ö., (1995), "Soot Morphology and Optical Properties in Nonpremixed Turbulent Flame Environments," Combustion Science and Technology **108**: 207-229.

Gülder, Ö. L., (1999), "Soot Particulate Formation and Characterization in Combustion," Transactions Of The Canadian Society For Mechanical Engineering **23**(1b): 225-240.

Hess, W. M. and Herd, C. R., (1993), "Microstructure, Morphology and General Physical Properties," in *Carbon Black Science and Technology*, Donnet, J.-B., Bansal, R. C. and Wang, M.-J., Eds., New York, Marcel Dekker, Inc.: 89-173.

Krishnan, S. S., Lin, K. C. and Faeth, G. M., (2000), "Optical Properties in the Visible of Overfire Soot in Large Buoyant Turbulent Diffusion Flames," Submitted to ASME Journal of Heat Transfer.

Leroy, O., Perrin, J., Jolly, J. and Pealat, M., (1997), "Thermal Accommodation of a Gas on Surface and Heat Transfer in CVD and PECVD Experiments," Journal of Physics D **30**: 499-509.

McCoy, B. J. and Cha, C. Y., (1974), "Transport Phenomena in the Rarefied Gas Transition Regime," Chemical Engineering Science **29**: 381-388.

McManus, K. R., Frank, J. H., Allen, M. G. and Rawlins, W. T., (1998), "Characterization of Laser-Heated Soot Particles Using Optical Pyrometry," AIAA Paper No. 98-0159, 36th Aerospace Sciences Meeting & Exhibit, Reno NV.

Melton, L. A., (1984), "Soot Diagnostics Based on Laser Heating," Applied Optics **23**(13): 2201-8.

Mewes, B. and Seitzman, J. M., (1997), "Soot Volume Fraction and Particle Size Measurements with Laser-Induced Incandescence," Applied Optics **36**(3): 709-717.

Ni, T., Pinson, J. A., Gupta, S. and Santoro, R. J., (1995), "Two-Dimensional Imaging of Soot Volume Fraction by the Use of Laser-Induced Incandescence," Applied Optics **34**(30): 7083-7091.

Quay, B., Lee, T. W., Ni, T. and Santoro, R. J., (1994), "Spatially Resolved Measurements of Soot Volume Fraction Using Laser-Induced Incandescence," Combustion and Flame **97**: 3-4.

Shaddix, C. R. and Smyth, K. C., (1996), "Laser-Induced Incandescence Measurements of Soot Production in Steady and Flickering Methane, Propane, and Ethylene Diffusion Flames," Combustion and Flame **107**: 418-452.

Smallwood, G. J., Snelling, D. R., Liu, F. and Gülder, Ö. L., (2000), "Clouds over Soot Evaporation: Errors in Modeling Laser-Induced Incandescence of Soot," submitted to Journal of Heat Transfer.

Smyth, K. C. and Shaddix, C. R., (1996), "Elusive History of m = 1.57 - 0.56i for the Refractive Index of Soot," Combustion and Flame **107**(3): 314-320.

Snelling, D. R., Smallwood, G. J., Campbell, I. G., Medlock, J. E. and Gülder, Ö. L., (1997), "Development and Application of Laser-Induced Incandescence (LII) as a Diagnostic for Soot Particulate Measurements," AGARD Conference Proceedings 598, Advanced Non-Intrusive Instrumentation for Propulsion Engines, Brussels, Belgium, 23-1 to 23-9.

Snelling, D. R., Smallwood, G. J., Sawchuk, R. A., Neil, W. S., Gareau, D., Chippior, W. L., Liu, F., Gülder, Ö. L. and Bachalo, W. D., (1999a), "Particulate Matter Measurements in a Diesel Engine Exhaust by Laser-Induced Incandescence and Standard Gravimetric Procedure," SAE Paper No. 1999-01-3653.

Snelling, D. R., Thomson, K. A., Smallwood, G. J. and Gülder, Ö. L., (1999b), "Two-Dimensional Imaging of Soot Volume Fraction in Laminar Diffusion Flames," Applied Optics **38**(12): 2478-2485.

Snelling, D. R., Liu, F., Smallwood, G. J. and Gülder, Ö. L., (2000a), "Evaluation of the Nanoscale Heat and Mass Transfer Model of the Laser-Induced Incandescence: Prediction of the Excitation Intensity," NHTC2000-12132, Thirty Fourth National Heat Transfer Conference, Pittsburgh, Pennsylvania.

Snelling, D. R., Smallwood, G. J., Sawchuk, R. A., Neil, W. S., Gareau, D., Clavel, D., Chippior, W. L., Liu, F., Gülder, Ö. L. and Bachalo, W. D., (2000b), "In-Situ Real-Time Characterization of Particulate Emissions from a Diesel Engine Exhaust by Laser-Induced Incandescence," SAE Paper No. 2000-01-1994.

Stagg, B. J. and Charalampopoulos, T. T., (1993), "Refractive Indices of Pyrolytic Graphite, Amorphous Carbon, and Flame Soot in the Temperature Range 25 Degree to 600 Degree C," Combustion and Flame **94**(4): 381-396.

Tait, N. P. and Greenhalgh, D. A., (1992), "2D Laser-Induced Fluorescence Imaging of Parent Fuel Fraction in Nonpremixed Combustion," 24th Symp. (Int.) on Combustion, 1621-1628.

Tait, N. P. and Greenhalgh, D. A., (1993), "PLIF Imaging of Fuel Fraction in Practical Devices and LII Imaging of Soot," Berichte der Bunsengesellschaft fuer Physikalische Chemie **97**(12): 1619-1625.

Vander Wal, R. L. and Dietrich, D. L., (1994), "Relative Soot Volume Fractions in Droplet Combustion Via Laser-Induced Incandescence," Chem. Phys. Processes Combust: 250-3.

Vander Wal, R. L. and Weiland, K. J., (1994), "Laser-Induced Incandescence: Development and Characterization Towards a Measurement of Soot-Volume Fraction," Applied Physics B **59**: 445-452.

Vander Wal, R. L., Choi, M. Y. and Lee, K.-O., (1995), "The Effects of Rapid Heating of Soot: Implications When Using Laser-Induced Incandescence for Soot Diagnostics," Combust. Flame **102**(1/2): 200-4.

Vander Wal, R. L. and Dietrich, D. L., (1995), "Laser-Induced Incandescence Applied to Droplet Combustion," Applied Optics **34**(6): 1103-1107.

Vander Wal, R. L., Zhou, Z. and Choi, M. Y., (1996), "Laser-Induced Incandescence Calibration Via Gravimetric Sampling," Combustion and Flame **105**: 462-470.

Vander Wal, R. L., Jensen, K. A. and Choi, M. Y., (1997), "Simultaneous Laser-Induced Emissions of Soot and Polycyclic Aromatic Hydrocarbons within a Gas-Jet Diffusion Flame," Combustion and Flame **109**: 399-414.

Vander Wal, R. L. and Jensen, K. A., (1998), "Laser-Induced Incandescence: Excitation Intensity," Applied Optics **37**(9): 1607-16.

Vander Wal, R. L., Ticich, T. M. and Stephens, A. B., (1998), "Optical and Microscopy Investigations of Soot Structure Alterations by Laser-Induced Incandescence," Applied Physics B (Lasers and Optics) **B67**(1): 115-23.

Vander Wal, R. L., Ticich, T. M. and Stephens, A. B., (1999), "Can Soot Primary Particle Size Be Determined Using Laser-Induced Incandescence?," Combustion and Flame **116**: 291-296.

Will, S., Schraml, S. and Leipertz, A., (1995), 'Two-Dimensional Soot-Particle Sizing by Time-Resolved Laser-Induced Incandescence," Optics Letters **20**(22): 2342-4.

Will, S., Schraml, S., Bader, K. and Leipertz, A., (1998), "Performance Characteristics of Soot Primary Particle Size Measurements by Time-Resolved Laser-Induced Incandescence.," Applied Optics **37**(24): 5647-5658.

Wu, J. S., Krishnan, S. K. and Faeth, G. M., (1996), "Refractive Indices at Visible Wavelengths of Soot Emitted from Buoyant Turbulent Diffusion Flames," Journal of Heat Transfer **119**: 230-237.